Electronic Supplementary Material (ESI) for Dalton Transactions.

Intense Multi-Colored Luminescence in a Series of Rare-Earth Metal-Organic Frameworks with Aliphatic Linkers

Pavel A. Demakov,[*a] Alexey A. Ryadun,[a] Pavel V. Dorovatovskii,[b] Vladimir A. Lazarenko,[b] Denis G. Samsonenko,[a] Konstantin A. Brylev,[a] Vladimir P. Fedin,[a] Danil N. Dybtsev[a]

[1] Nikolaev Institute of Inorganic Chemistry, Siberian Branch of the Russian Academy of Sciences, Novosibirsk 630090, Russia

[2] National Research Centre "Kurchatov Institute", Kurchatov Square 1, Moscow 123182, Russia

Supporting Information

Table of contents

1. Experimental and Crystallography Details.

General Remarks. Trans-1,4-cyclohexanedicarboxylic acid (H_2chdc, >97.0%), 2,2'-bipyridyl (bpy, >99.0%) and 1,10-phenanthroline monohydrate (phen·H_2O, >98.0%) were received from TCI. $Y(NO_3)_3 \cdot 6H_2O$ (99.9% REO) and $Eu(NO_3)_3 \cdot 6H_2O$ (99.9% REO) were received from Dalchem. N,N-dimethylformamide (DMF, reagent grade), $Tb(NO_3)_3 \cdot 5H_2O$ (reagent grade), $TbCl_3 \cdot 6H_2O$ (reagent grade), $EuCl_3 \cdot 6H_2O$ (reagent grade) were received from Vekton. $YCl_3 \cdot 6H_2O$ was received from Reachem. All reagents were used as received without further purification. As determined by ICP-MS, the starting $YCl_3 \cdot 6H_2O$ contained 0.5% (molar) of Tb. IR spectra in KBr pellets were recorded in the range 4000−400 cm^{-1} on a Bruker Scimitar FTS 2000 spectrometer. Elemental analysis was made on a VarioMICROcube analyzer. Powder X-ray diffraction (PXRD) analysis was performed at room temperature on a Shimadzu XRD-7000 diffractometer (Cu-Kα radiation, λ = 1.54178 Å). In-situ PXRD in 25 – 300 °C temperature range was performed at room STOE STADI-P diffractometer (Co-Kα radiation, λ = 1.78897 Å) equipped with Ultima IV goniometer. Thermogravimetric analysis was carried out using a Netzsch TG 209 F1 Iris instrument under Ar flow (30 $cm^3 \cdot min^{-1}$) at a 10 $K \cdot min^{-1}$ heating rate. Excitation and emission photoluminescence spectra were recorded with a spectrofluorometer Horiba Jobin Yvon Fluorolog 3 equipped with ozone-free Xe-lamp 450W power, cooled photon detector R928/1860 PFR technologies with refrigerated chamber PC177CE-010 and double grating monochromators. Excitation and emission spectra were corrected for source intensity and detector spectral response by standard correction curves. The absolute quantum yield was measured using a G8 (GMP SA, Switzerland) spectralon-coated integrating sphere, which was connected to a Fluorolog 3 spectrofluorimeter. ICP-MS analysis was carried out on Agilent 8800 device. The samples were digested in the mixture of HCl 36% water solution and H_2O_2 30% water solution, then diluted by water prior to ICP-MS.

Single crystal X-Ray diffraction analysis details. Diffraction data for single crystals of **1–3** were obtained on an automated Agilent Xcalibur diffractometer equipped with an area AtlasS2 detector (graphite monochromator, λ(MoKα) = 0.71073 Å, ω-scans with a step of 0.5°). Integration, absorption correction, and determination of unit cell parameters were performed using the CrysAlisPro program package.[1] Diffraction data for single crystals of **4–6** were collected on the 'Belok' beamline (λ = 0.79272 Å for **4** and **5**; λ = 0.79475 Å for **6**; φ-scans with a step of 1.0°) of the National Research Center 'Kurchatov Institute' (Moscow, Russian Federation) using a Rayonix SX165 CCD detector. The data were indexed, integrated and scaled, absorption correction was applied using the XDS program package.[2] The structures were solved by dual space algorithm (SHELXT[3]) and refined by the full-matrix least squares

technique (SHELXL[4]) in the anisotropic approximation (except hydrogen atoms). Positions of hydrogen atoms of organic ligands were calculated geometrically and refined in the riding model. The crystallographic data and details of the structure refinements are summarized in Tables S1 and S2. CCDC 2024826–2024831 contain the supplementary crystallographic data for this paper. These data can be obtained free of charge from The Cambridge Crystallographic Data Center at https://www.ccdc.cam.ac.uk/structures/.

Table S1. X-Ray structure determination details for **1–3**.

	1	**2**	**3**
Chemical formula	$C_{44}H_{46}N_4O_{12}Y_2$	$C_{44}H_{46}Eu_2N_4O_{12}$	$C_{44}H_{47}N_4O_{12.5}Tb_2$
M_r	1000.67	1126.77	1149.69
Crystal system	Monoclinic	Monoclinic	Monoclinic
Space group	$P2_1/n$	$P2_1/n$	$P2_1/n$
Temperature (K)	130	150	130
a, *b*, *c* (Å)	10.3847 (6) 17.547 (1) 12.2030 (6)	10.4401 (3) 17.6295 (5) 12.3060 (4)	10.4023 (5) 17.5671 (8) 12.2985 (8)
β (°)	103.354 (5)	103.832 (3)	103.709 (6)
V (Å^3)	2163.5 (2)	2199.28 (12)	2183.4 (2)
Calc. density (g cm^{-1})	1.536	1.701	1.749
Z	2	2	2
F(000)	1024	1120	1138
μ (mm^{-1})	2.74	2.89	3.28
Crystal size (mm)	0.12 × 0.05 × 0.03	0.10 × 0.04 × 0.02	0.21 × 0.05 × 0.03
h, k, l indices range	-13 < h < 14 -13 < k < 22 -16 < l < 8	-13 < h < 14 -21 < k < 21 -16 < l < 16	-12 < h < 14 -20 < k < 24 -16 < l < 11
No. of measured, independent and observed [$I > 2\sigma(I)$] reflections	11750 5117 4462	11086 4836 4139	12350 5212 4452
R_{int}	0.028	0.028	0.024
$R[F^2 > 2\sigma(F^2)]$	0.029	0.029	0.022
R[all data]	0.039	0.039	0.032
$wR[F^2 > 2\sigma(F^2)]$	0.060	0.043	0.043
$wR(F^2)$	0.062	0.045	0.045
Goodness of fit	1.05	1.03	1.02
$\Delta\rangle_{max}$, $\Delta\rangle_{min}$ (e Å^{-3})	0.42, -0.37	0.72, -0.56	0.64, -0.88

Table S2. X-Ray structure determination details for **4**–**6**.

	4	**5**	**6**
Chemical formula	$C_{49.5}H_{49.5}N_{4.5}O_{12.5}Y_2$	$C_{49.5}H_{49.5}Eu_2N_{4.5}O_{12.5}$	$C_{49.5}H_{49.5}N_{4.5}O_{12.5}Tb_2$
M_r	1085.25	1211.35	1225.27
Crystal system	Monoclinic	Monoclinic	Monoclinic
Space group	$P2_1/n$	$P2_1/n$	$P2_1/n$
Temperature (K)	100	100	100
a, *b*, *c* (Å)	10.334 (4) 17.831 (3) 12.7530 (14)	10.423 (10) 17.902 (9) 12.892 (7)	10.411 (2) 17.893 (3) 12.831 (2)
β (°)	98.75 (5)	99.11 (4)	98.908 (3)
V (Å^3)	2322.6 (11)	2375 (3)	2361.4 (7)
Calc. density (g cm^{-1})	1.552	1.694	1.723
Z	2	2	2
F(000)	1112	1208	1216
μ (mm^{-1})	0.63	3.55	4.05
Crystal size (mm)	0.04 × 0.02 × 0.02	0.06 × 0.04 × 0.02	0.05 × 0.03 × 0.02
h, k, l indices range	-13 < h < 13 -23 < k < 23 -16 < l < 16	-13 < h < 10 -23 < k < 23 -13 < l < 16	-13 < h < 12 -23 < k < 23 -16 < l < 16
No. of measured, independent and observed [$I > 2\sigma(I)$] reflections	26174 5306 3475	12044 5239 4611	19162 5388 3922
R_{int}	0.096	0.073	0.064
$R[F^2 > 2\sigma(F^2)]$	0.064	0.051	0.044
R(all data)	0.102	0.059	0.070
$wR[F^2 > 2\sigma(F^2)]$	0.162	0.129	0.105
wR(all data)	0.181	0.137	0.115
Goodness of fit	1.03	1.05	1.03
$\Delta\rangle_{max}$, $\Delta\rangle_{min}$ (e Å^{-3})	0.83, -1.00	1.14, -1.73	0.91, -1.06

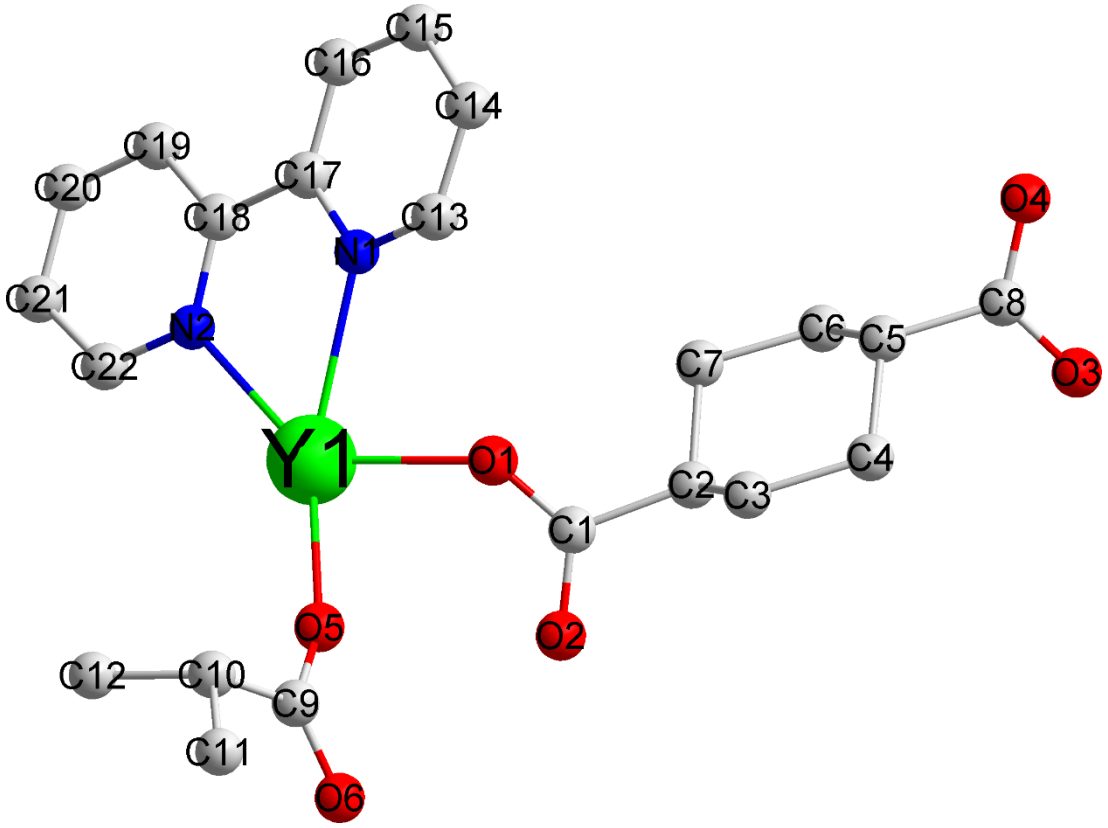

Figure S1. Atom numbering scheme in **1**.

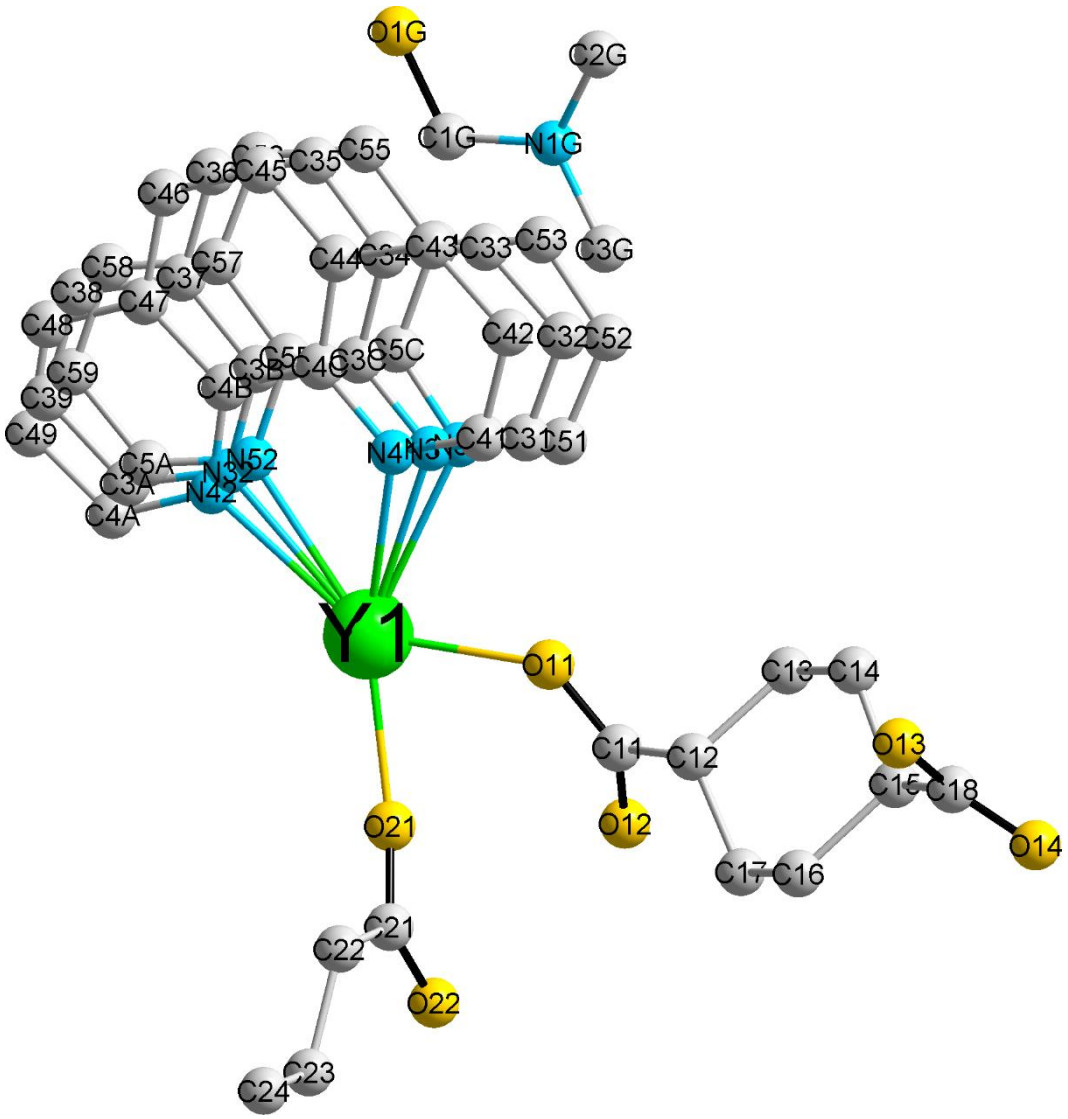

Figure S2. Atom numbering scheme in **4**.

2. PXRD data

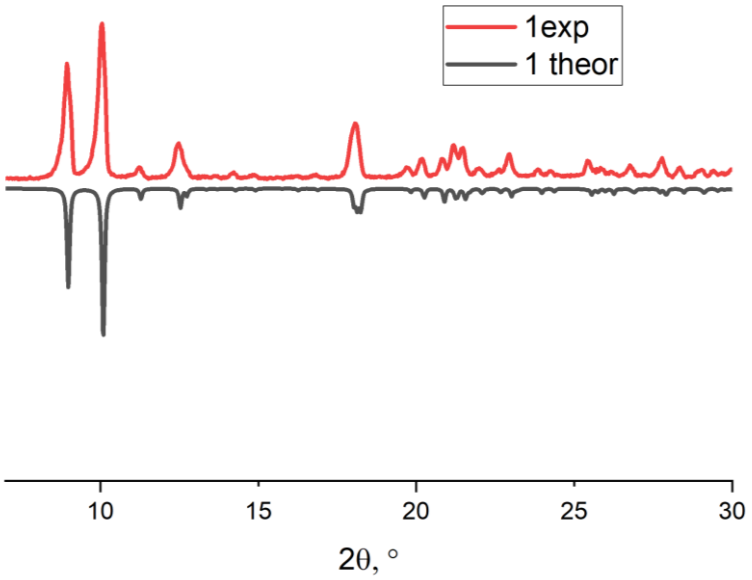

Figure S3. PXRD pattern of the synthesized **1** sample (red line) compared to the theoretical diffractogram (black line).

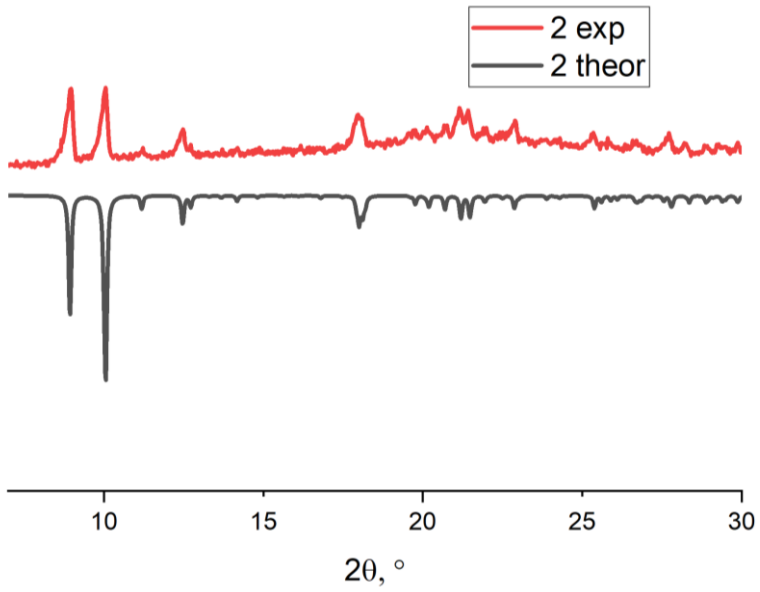

Figure S4. PXRD pattern of the synthesized **2** sample (red line) compared to the theoretical diffractogram (black line).

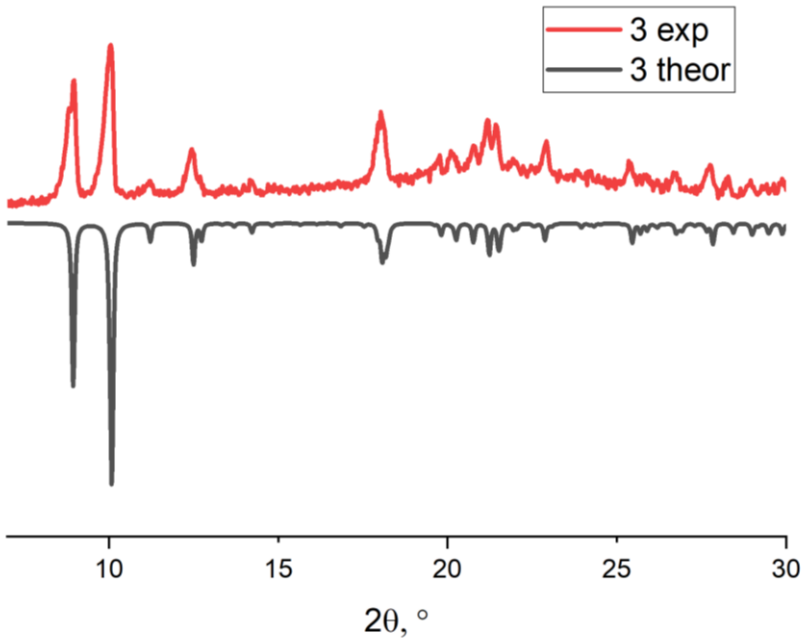

Figure S5. PXRD pattern of the synthesized **3** sample (red line) compared to the theoretical diffractogram (black line).

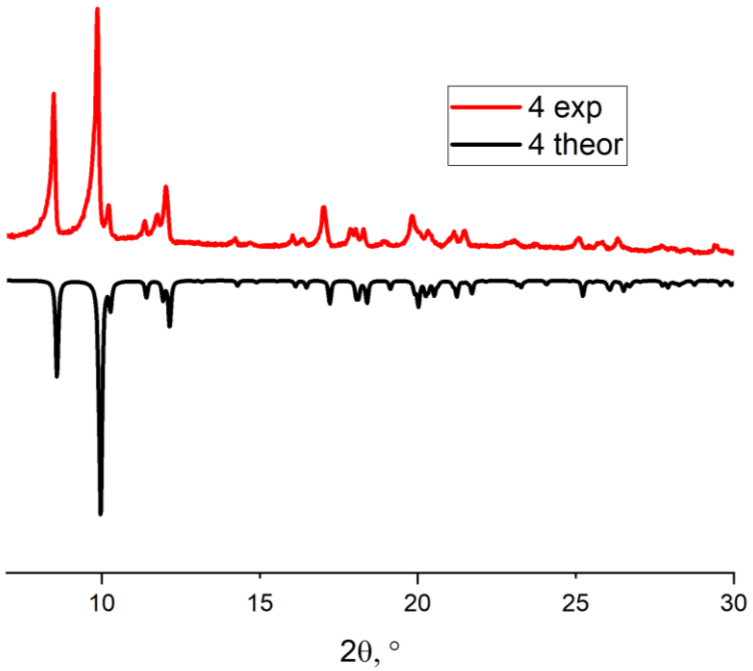

Figure S6. PXRD pattern of the synthesized **4** sample (red line) compared to the theoretical diffractogram (black line).

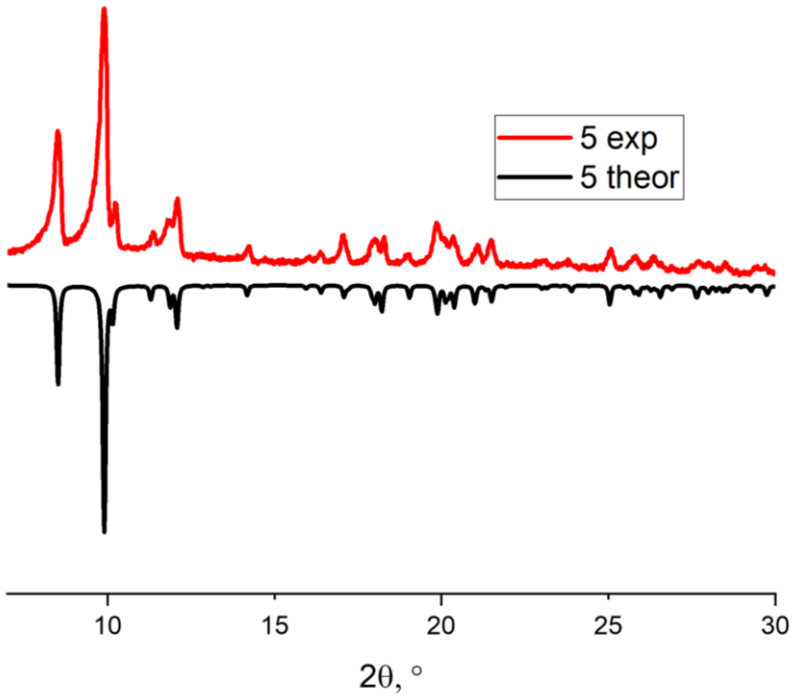

Figure S7. PXRD pattern of the synthesized **5** sample (red line) compared to the theoretical diffractogram (black line).

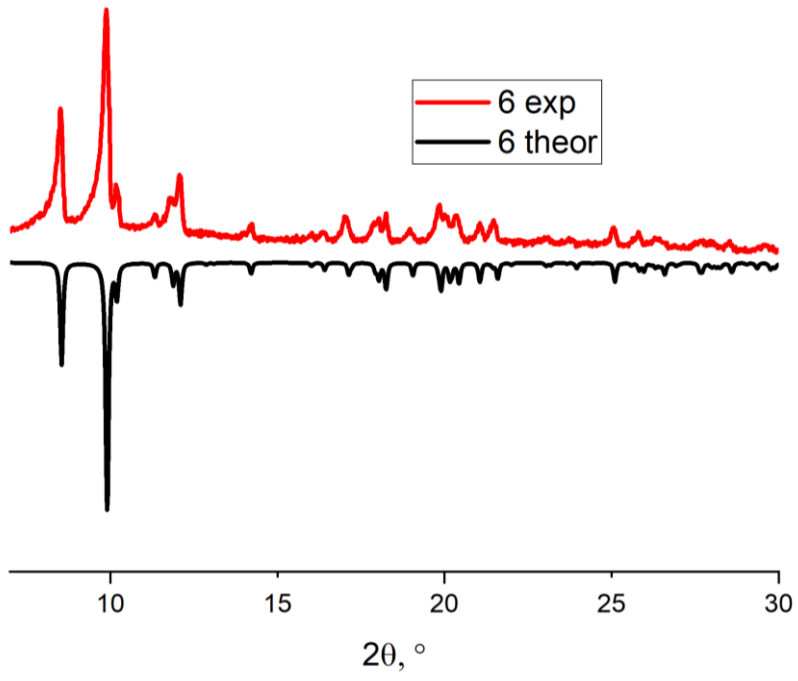

Figure S8. PXRD pattern of the synthesized **6** sample (red line) compared to the theoretical diffractogram (black line).

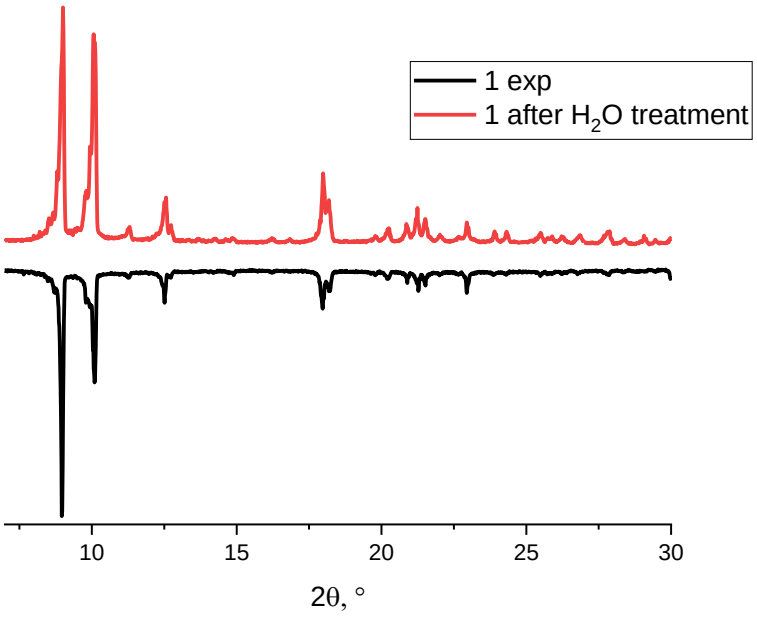

Figure S9. PXRD pattern of the water-treated sample of **1** (red line) compared to the as-synthesized **1** (black line).

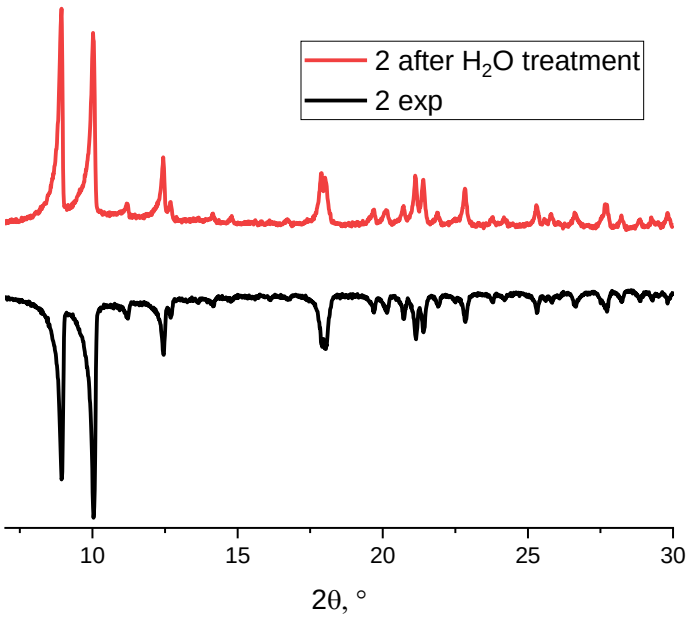

Figure S10. PXRD pattern of the water-treated sample of **2** (red line) compared to the as-synthesized **2** (black line).

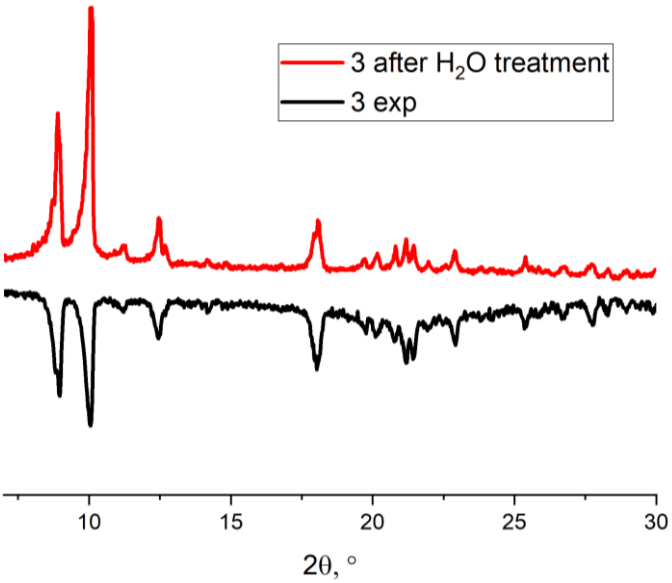

Figure S11. PXRD pattern of the water-treated sample of **3** (red line) compared to the as-synthesized **3** (black line).

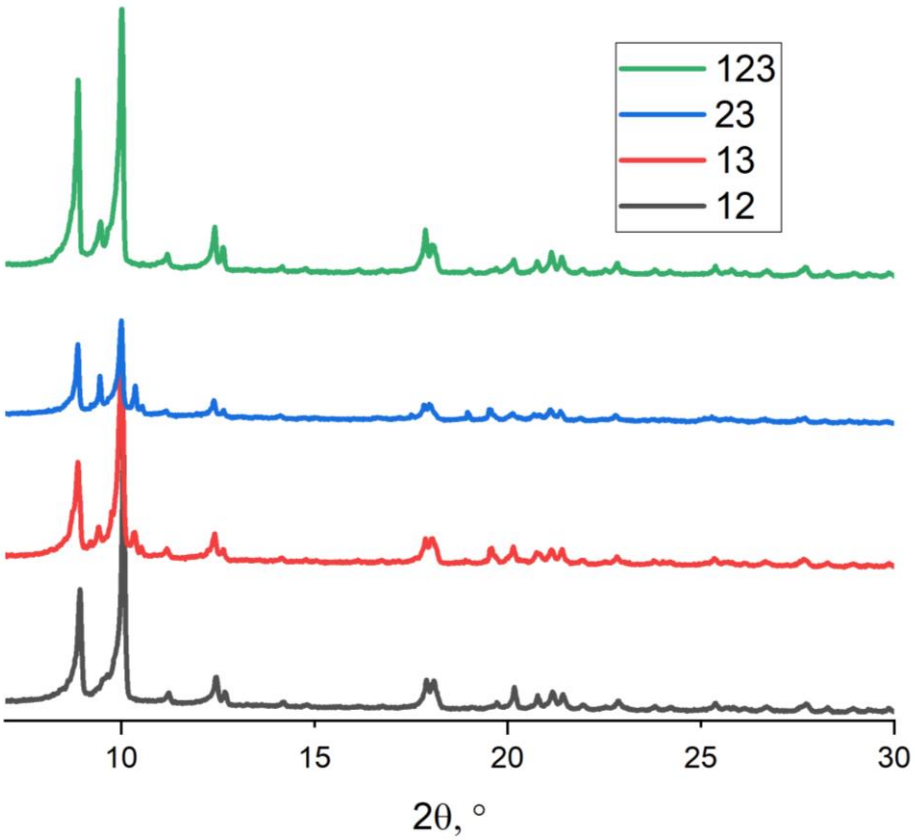

Figure S12. PXRD patterns of the mixed-metal samples **12**, **13**, **23** and **123**.

3. IR spectra

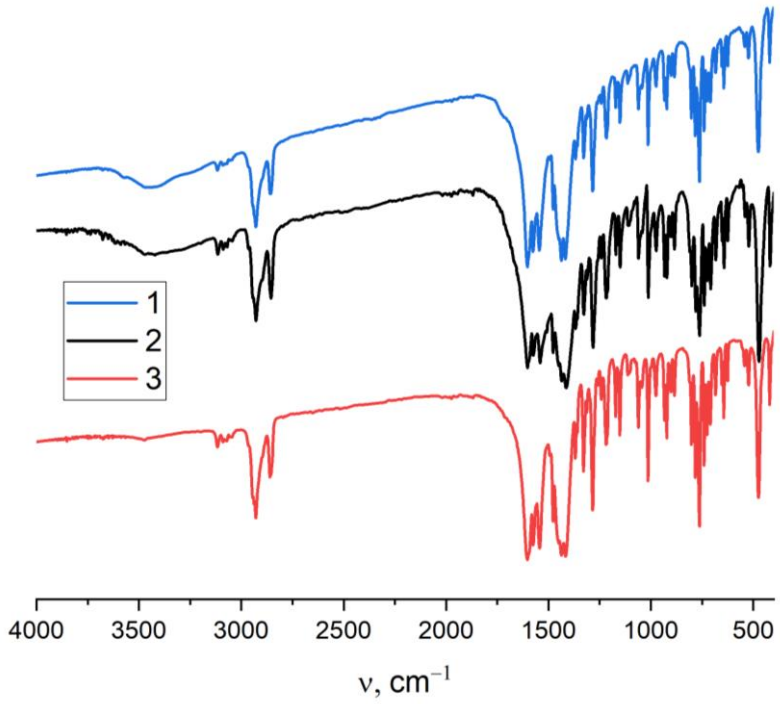

Figure S13. IR spectra of the compounds **1** – **3**.

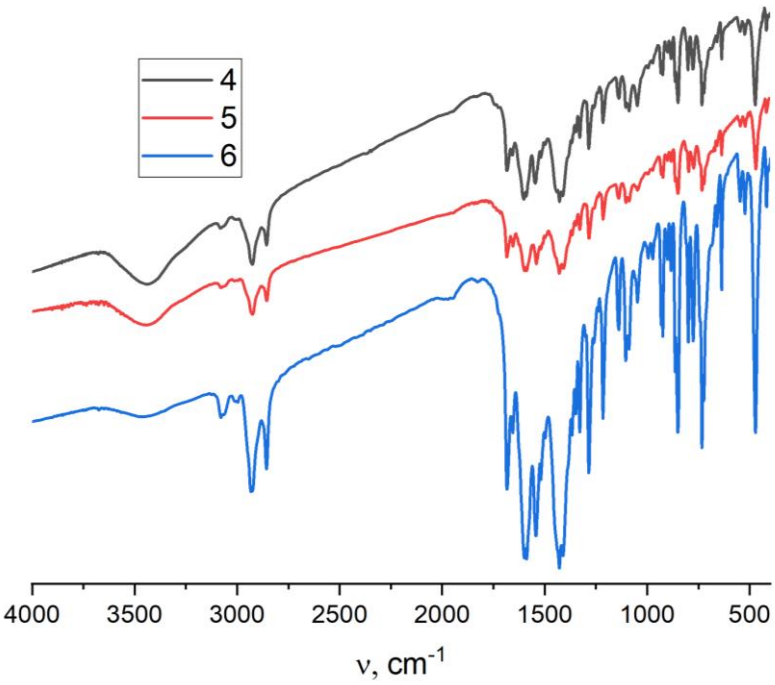

Figure S14. IR spectra of the compounds **4** – **6**.

4. Thermal stability data

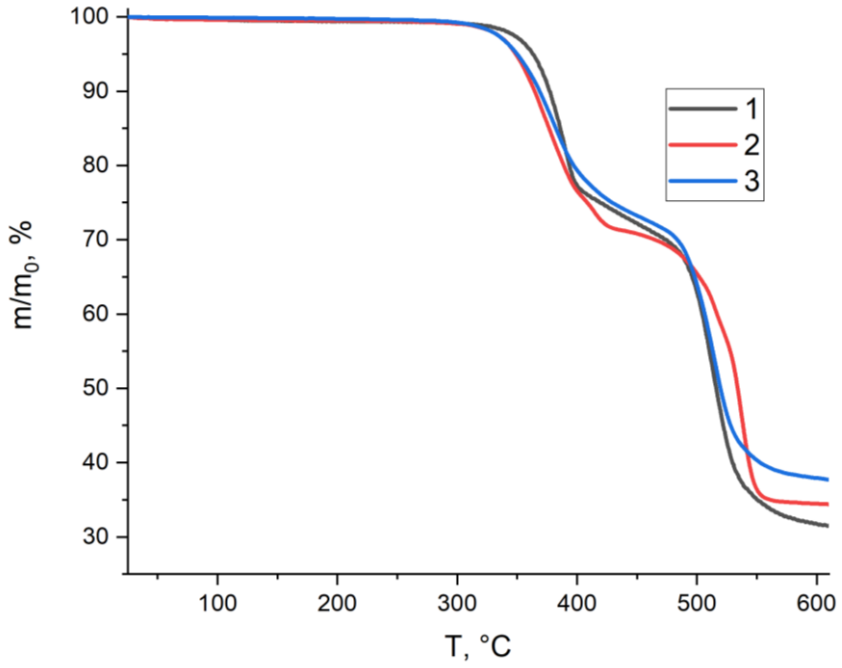

Figure S15. TG plots for the compounds **1** – **3**.

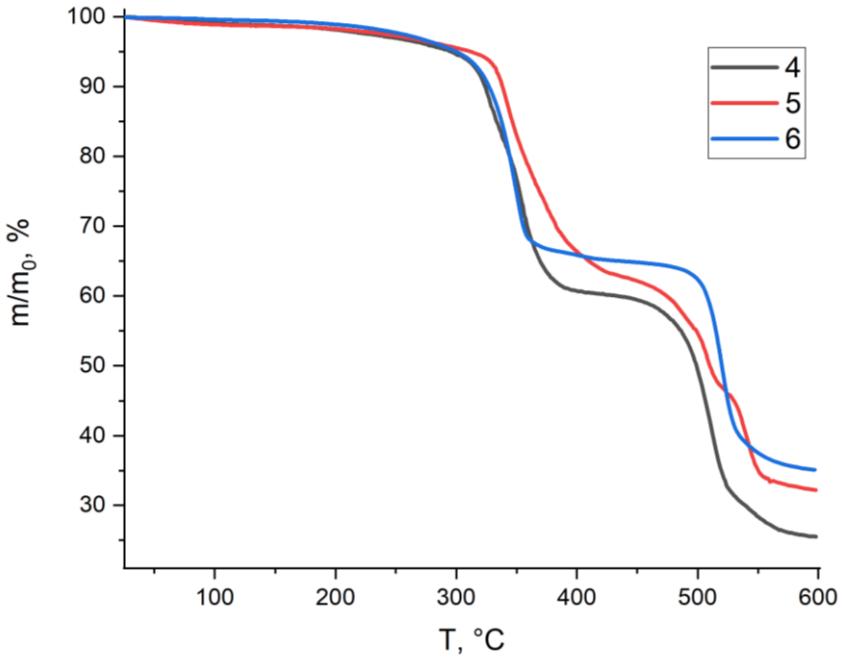

Figure S16. TG plots for the compounds **4** – **6**.

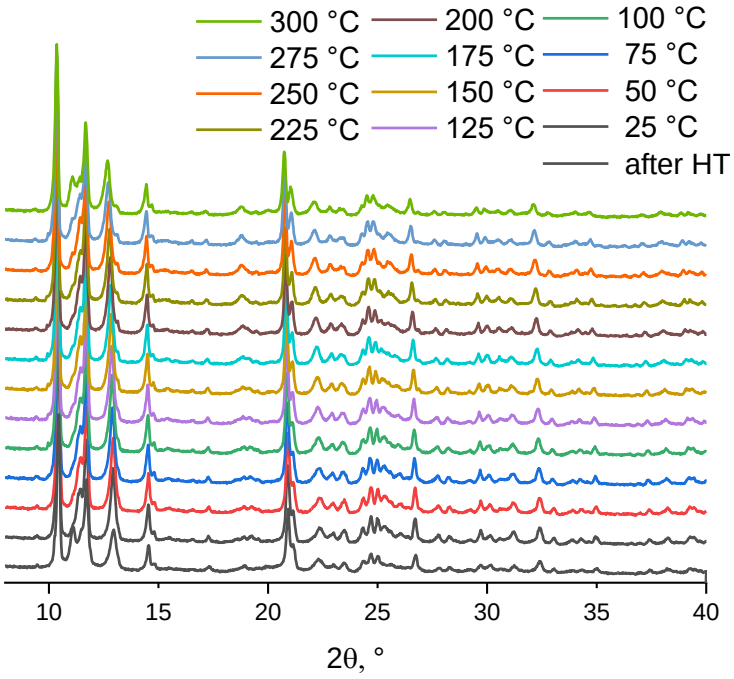

Figure S17. In-situ PXRD patterns for **1** in the temperature range 25 – 300 °C.

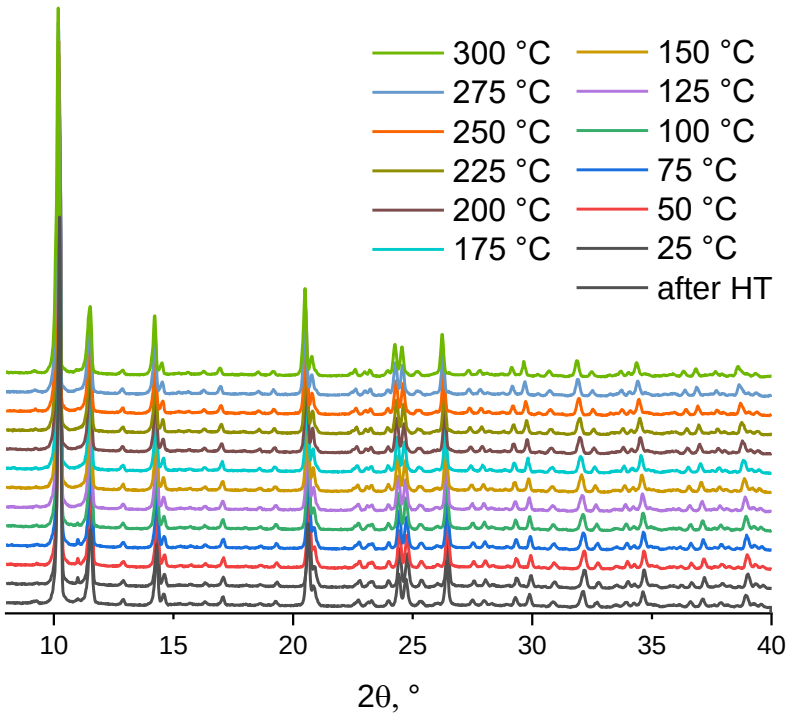

Figure S18. In-situ PXRD patterns for **2** in the temperature range 25 – 300 °C.

5. Luminescence supplementary data

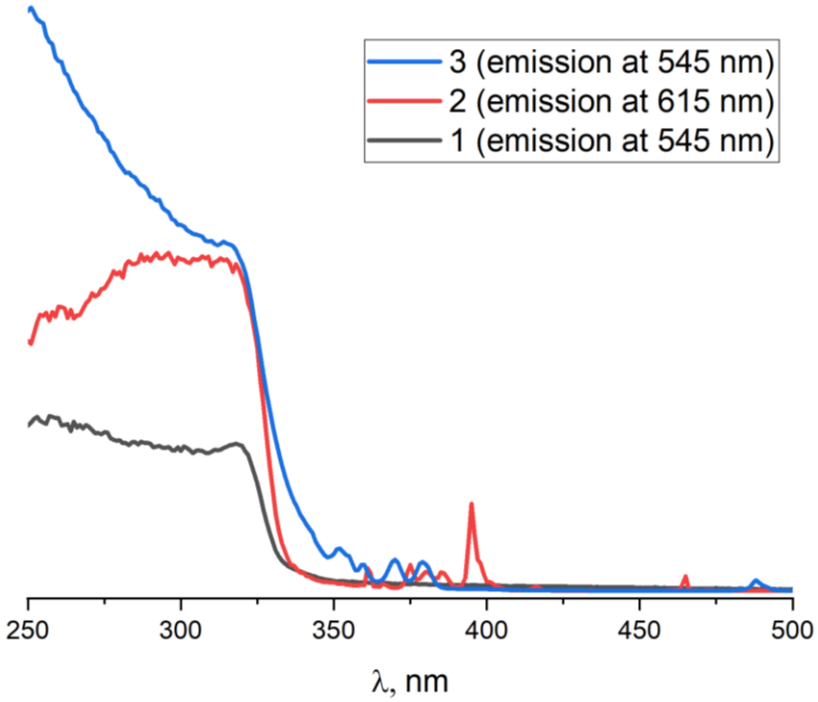

Figure S19. Excitation spectra of the compounds **1 - 3**.

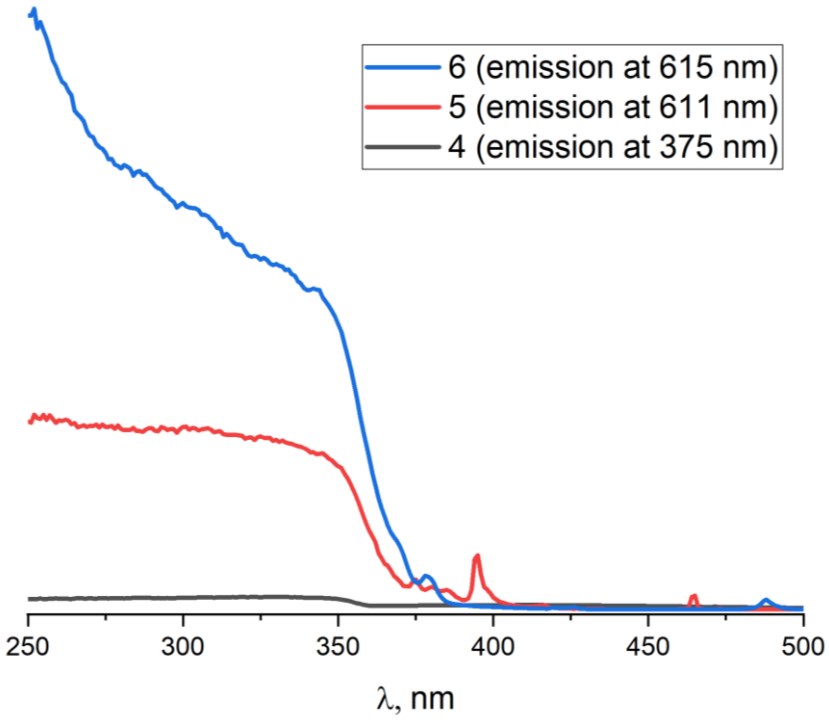

Figure S20. Excitation spectra of the compounds **4 - 6**.

Table S3. The calculated emission characteristic wavelengths and color purity values for the individual compounds **1 – 6**.

Sample	Emission region	Characteristic wavelength λ_{em}, nm	Color purity, %
1	Blue	465	87.1
4		472	77.4
2	Red	607	99.8
5		606	100.0
3	Green	560	82.2
6		561	83.2

Table S4. Chemical formulae and emission quantum yields of the reported Ln^{3+} metal-organic frameworks with N-donor chelate ligands comprising 2,2′-bipyridyl core (bpy, phen and their homologs).

Formula	Metal center	QY, %	λ_{ex}, nm	Reference
$[HNMe_2][Tb_2(m\text{-}BDC)_3(phen)_2]$	Tb^{3+}	85.62	345	[5]
$[Tb(ppmc)_3(phen)]$	Tb^{3+}	65.6	352	[6]
$[Tb_2(bpy)_2(chdc)_3]\cdot 0.5H_2O$	Tb^{3+}	**59**	345	**This work**
$[Tb_2(phen)_2(chdc)_3]\cdot 0.5DMF$	Tb^{3+}	**49**	345	**This work**
$[Tb(Hdpstc)(phen)(H_2O)]_n\cdot 1.5nH_2O$	Tb^{3+}	48.05	329	[7]
$[Tb_2(2,3'\text{-}oba)_3(phen)_2]$	Tb^{3+}	41.86	365	[8]
$[Tb(2,6\text{-}Nds)_{0.5}(ox)(phen)(H_2O)]$	Tb^{3+}	30.54	271	[9]
$[Tb(Hdpstc)(H_2O)_2]\cdot H_2O$	Tb^{3+}	26.05	302	[7]
[Tb(μ-HL)(μ3-L)(phen)]	Tb^{3+}	22.1	320	[10]
$[Tb_3L_9]\cdot 0.5H_2O$	Tb^{3+}	17.4	332	[11]
$[Tb(3,4'\text{-}oba)(phen)_2(ox)_{0.5}]$	Tb^{3+}	10.30	338	[12]
[Tb(ppmdc)(benzoate)(phen)]	Tb^{3+}	9.5	346	[6]
$[Tb(ADA)_{1.5}(phen)]$	Tb^{3+}	9.07	345	[13]
$[Tb(ppmc)_2(C_2O_4)_{0.5}(H_2O)]$	Tb^{3+}	3.4	324	[6]
$[Tb_2(ADA)_3(dmp)_2]\cdot 2EtOH\cdot H_2O$	Tb^{3+}	0.34	332	[14]
$[HNMe_2][Ln_2(m\text{-}BDC)_3(phen)_2]$	Eu^{3+}	86.87	330	[5]
$[Ln_2(2,3'\text{-}oba)_3(phen)_2]$	Eu^{3+}	75.57	365	[8]
$[(Y,Eu)_2(phen)_2(fdc)_3(H_2O)_2]$	$\underline{Eu^{3+}}$, Y^{3+}	66	344	[15]
$[(Y,Eu)_2(phen)_2(fdc)_3]$	$\underline{Eu^{3+}}$, Y^{3+}	64	344	[15]
$[Ln(ADA)_{1.5}(phen)]$	Eu^{3+}	58.61	345	[13]
$[Ln_3L_9]\cdot 0.5H_2O$	Eu^{3+}	58.4	332	[11]
$[Eu_2(phen)_2(chdc)_3]\cdot 0.5DMF$	Eu^{3+}	**55**	345	**This work**
$[EuL(CH_3COO)Cl]$	Eu^{3+}	48.82	361	[16]
[Ln(μ-HL)(μ3-L)(phen)]	Eu^{3+}	48.4	348	[10]
$[Eu_2(bpy)_2(chdc)_3]$	Eu^{3+}	**46**	345	**This work**
$[Ln(ppmc)_3(phen)]$	Eu^{3+}	43.9	346	[6]
$[Ln(3,4'\text{-}oba)(phen)_2(ox)_{0.5}]$	Eu^{3+}	40.51	332	[12]
[Eu(NCP)(ndc)]	Eu^{3+}	39	396	[17]
$[Ln(1,5\text{-}Nds)_{0.5}(ox)(phen)(H_2O)]\cdot H_2O$	Eu^{3+}	38.91	358	[9]
$[Ln(Hdpstc)(phen)(H_2O)]\cdot 1.5H_2O$	Eu^{3+}	35.74	365	[7]
$[Ln_2(ADA)_3(dmp)_2]\cdot 2EtOH\cdot H_2O$	Eu^{3+}	32	332	[14]
$[Ln(2,6\text{-}Nds)_{0.5}(ox)(phen)(H_2O)]$	Eu^{3+}	28.29	329	[9]

$[Eu(NCP)(ndc)]\cdot 2H_2O$	Eu^{3+}	26	396	[17]
$[Tb_{1-x}Eu_x(BDC)_{0.5}(DSTP)]\cdot 2H_2O$	Tb^{3+}, Eu^{3+}	24.5	360	[18]
[Eu(NCP)(4,4′-bpdc)]	Eu^{3+}	18	396	[17]
$[Tb_{1-x}Eu_x(OA)_{0.5}(DSTP)]\cdot 3H_2O$	Tb^{3+}, Eu^{3+}	16.2	360	[18]
$[Eu(ppmdc)(phen)(C_2O_4)_{0.5}]\cdot H_2O$	Eu^{3+}	13.4	336	[6]
$[Ln(Hdpstc)(H_2O)_2]\cdot H_2O$	Eu^{3+}	11.19	365	[7]
[Eu(NCP)(1,4-bdc)]	Eu^{3+}	11	396	[17]
$[Ln(ppmc)_2(C_2O_4)_{0.5}(H_2O)]$	Eu^{3+}	10.2	343	[6]
[Ln(TMAla)(HTMAla)(phen)]	Eu^{3+}	5.34	358	[19]
$[Eu(NCP)(2,5\text{-}Br_2bdc)]$	Eu^{3+}	4	396	[17]
$[Y_2(bpy)_2(chdc)_3]$	Y^{3+}	**63**	300	**This work**
$[Y_2(phen)_2(chdc)_3]\cdot 0.5DMF$	Y^{3+}	**2.3**	320	**This work**
$[LnLIJglu)]\cdot 2H_2O$	Y^{3+}	not reported	370	[20]
$[Y_2(C_{12}N_2H_8)_2(1,2\text{-BDC})_2(1,3\text{-BDC})]$	Y^{3+}	not reported	327	[21]
$[Y_2(C_{12}N_2H_8)_2(1,2\text{-BDC})_2(1,4\text{-BDC})]$	Y^{3+}	not reported	330	[21]
$[Y_2(C_{12}N_2H_8)_2(C_8H_4O_4)_3]\cdot H_2O$	Y^{3+}	not reported	-	[22]
$[Y_2(C_{12}N_2H_8)_2(C_8H_4O_4)_3]$	Y^{3+}	not reported	-	[22]
$[Ln(Hsfpip)(ox)_{0.5}(H_2O)]\cdot 2H_2O$	Y^{3+}	not reported	-	[23]

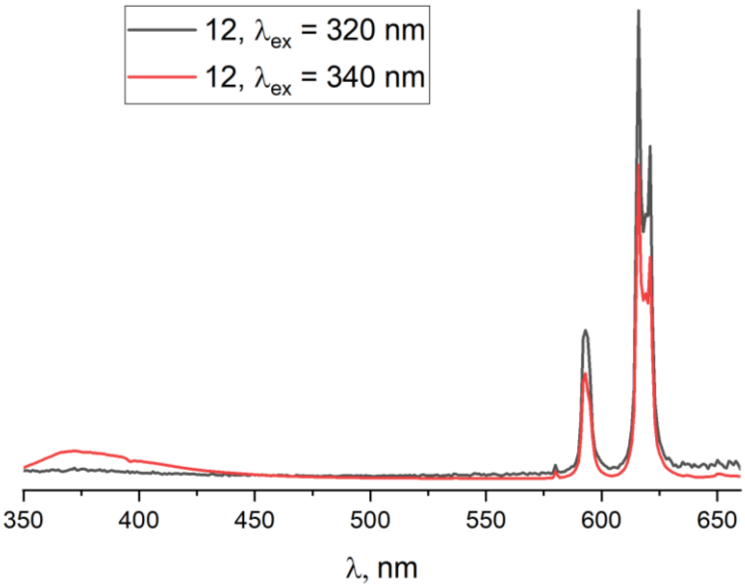

Figure S21. Emission spectra of the sample **12** at λ_{ex}= 320 nm (black line) and at λ_{ex}= 340 nm (red line)

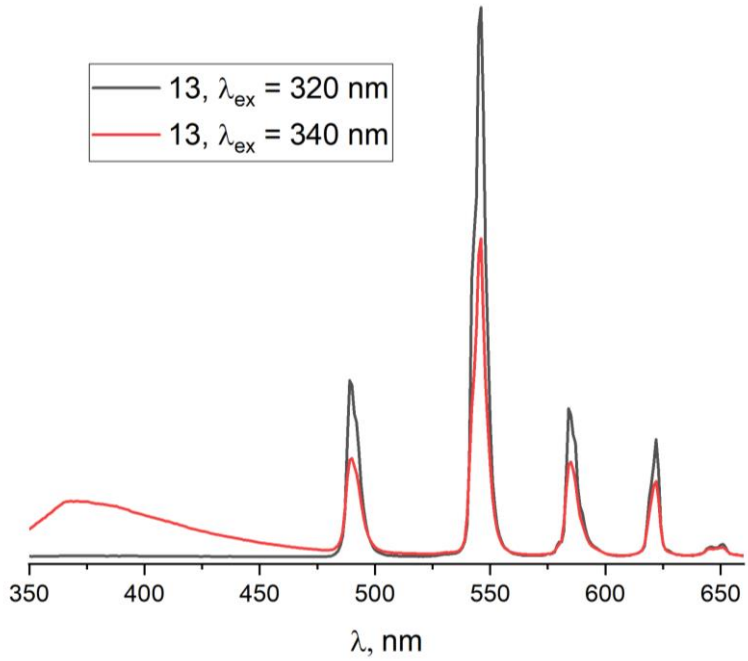

Figure S22. Emission spectra of the sample **13** at λ_{ex}= 320 nm (black line) and at λ_{ex}= 340 nm (red line)

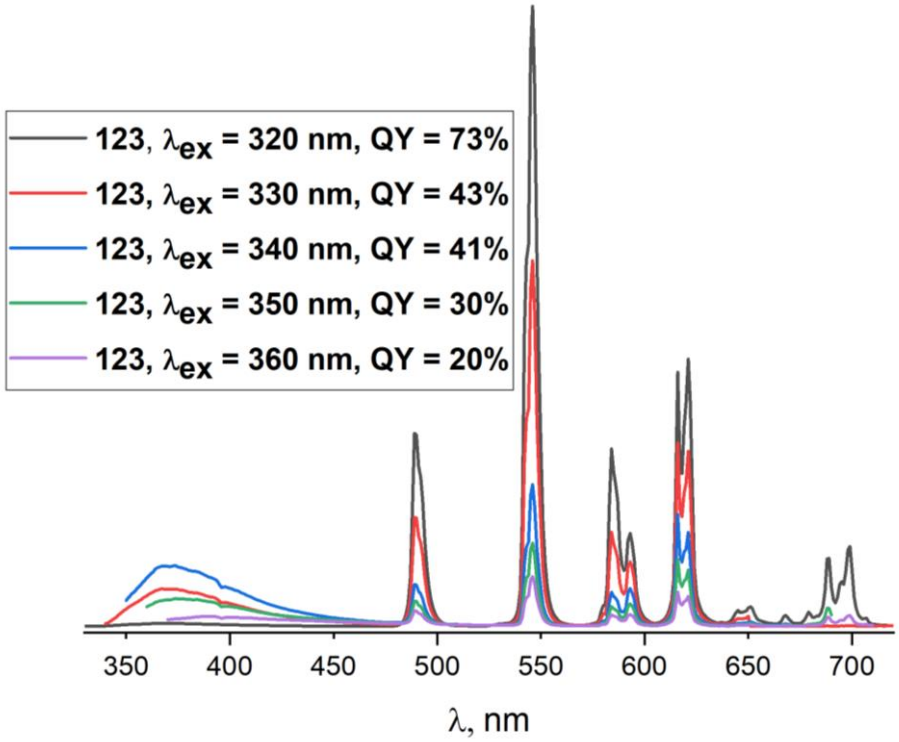

Figure S23. Emission spectra of the sample **123** at different wavelengths and corresponding quantum yields.

Table S5. The calculated emission characteristic wavelengths and color purity values for the mixed-metal sample **123** at different excitation wavelengths

λ_{ex}, nm	Characteristic wavelength λ_{em}, nm	Color purity, %
320	570	87.5
330	575	62.8
340	583	26.0
350	582	11.5
360	576	5.6

Table S6. Chemical formulae and quantum yields of the reported white emitters based on Ln^{3+} metal-organic frameworks with N-donor chelate ligands comprising 2,2′-bipyridyl core (bpy, phen and their homologs).

Formula	Metal center	QY, %	λ_{ex}, nm	Reference
$[Ln(oba)phen(ox)_{0.5}]$	Gd^{3+}, Eu^{3+}, Tb^{3+}	38.74	370	[24]
$[Ln_2(m\text{-}BDC)_3(phen)_2]\cdot DMF$	Gd^{3+}, Eu^{3+}, Tb^{3+}	32	350	[25]
$[Ln_2(bpy)_2(chdc)_3]$	Y^{3+}, Eu^{3+}, Tb^{3+}	**20**	360	**This work**
[Ln(MBDC)(STP)]	La^{3+}, Eu^{3+}	12	390	[26]
$[Ln(3\text{-}SBA)(IP)OH(H_2O)]\cdot H_2O$	Gd^{3+}, Eu^{3+}	9.92	388-390	[27]
$[LnL(glu)]\cdot 2H_2O$	Eu^{3+}, Tb^{3+}	6.03	370	[28]
$[Ln(4\text{-}SBA)(IP)OH]\cdot 1.5H_2O$	Sm^{3+}, Eu^{3+}	3.40	370	[29]
$[Ln(4\text{-}SBA)(IP)OH]\cdot 1.5H_2O$	Sm^{3+}, Gd^{3+}, Eu^{3+}	2.23	390	[29]
$[Ln_2(TFPht)_3(phen)_2(H_2O)_2]\cdot H_2O$	Dy^{3+}, Gd^{3+}, Eu^{3+}	2.10	347	[30]
$[Ln_2(TFPht)_3(phen)_2(H_2O)_2]\cdot H_2O$	Dy^{3+}, Eu^{3+}	1.23	352	[30]
[Ln(Fpht)(HFpht)(phen)(H_2O)]	La^{3+}, Eu^{3+}, Tb^{3+}	not reported	370	[31]
$[Ln_2(TDA)_3(bipy)_2(H_2O)_2]\cdot bipy\cdot 2H_2O$	Eu^{3+}	not reported	324	[32]
$[Ln_2(MPIP)_2(1,3\text{-}bdc)_3]\cdot xH_2O$	La^{3+}, Eu^{3+}, Tb^{3+}	not reported	360	[33]
$[Ln(cphtH)phen(ox)_{0.5}]\cdot mH_2O$	Sm^{3+}	not reported	356	[34]
[Ln(Hbtca)(phen)]	Eu^{3+}, Tb^{3+}	not reported	360	[35]

6. References

1. CrysAlisPro 1.171.38.46. Rigaku Oxford Diffraction: The Woodlands, TX, USA, 2015

2. W. Kabsch, XDS. *Acta Crystallogr*.. 2010, **D66**, 125.

3. G. M. Sheldrick, SHELXT - Integrated space-group and crystal-structure determination, *Acta Crystallogr*., 2015, A71, 3.

4. G. M. Sheldrick, Crystal structure refinement with SHELXL, *Acta Crystallogr*., 2015, C71, 3.

5. H.-B. Zhang, Y. Peng, X.-C. Shan, C.-B. Tian, P. Lin, S.-W. Du, Lanthanide metal organic frameworks based on octahedral secondary building units: Structural, luminescent, and magnetic properties, *Inorg. Chem. Comm*., 2011, **14**, 1165.

6. L. Jia, Y.-C. Hui, Z. Li, H.-L. Sun, Z. Wang, Luminescent Lanthanide-2-phenylpyrimidine-carboxylate Frameworks: Structure and Luminescence Tuning, *CrystEngComm*, 2014, **16**, 6483.

7. C.-T. Li, Y.-F. Zhao, H.-M. Hu, H. Zhao, X. Wang, G. Xue, Lanthanide coordination frameworks constructed from 3,3’,4,4’-diphenylsulfonetetracarboxylic and 1,10-phenanthroline: synthesis, crystal structures and luminescence properties, *Dalton Trans*., 2016, **45**, 15436.

8. J.-M. Li, R. Li, X. Li, Construction of metal-organic frameworks (MOFs) and Highly luminescent Eu(III)-MOF for detection of inorganic ions and antibiotics in aqueous medium, *CrystEngComm*, 2018, **20**, 4962.

9. R. Li, X.-L. Qu, Y.-H. Zhang, H.-L. Han, X. Li, Lanthanide- organic frameworks constructed from naphthalenedisulfonate: Structure, luminescence and luminescent sensing properties, *CrystEngComm*, 2016, **18**, 5890.

10. J. Wang, Q.-S. Zhang, W. Dou, A. M. Kirillov, W.-S. Liu, C. Xu, C.-L. Xu, R. Fang, L. Yang, Novel Double Layer Lanthanide Metal-Organic Networks for Sensing Applications, *Dalton Trans*., 2018, **47**, 465.

11. P. Lin, F. Jiang, M. Wu, M. Hong, Syntheses, structures, photoluminescence and magnetic properties of 1D lanthanide chains featuring 2,2′-bipyridine-5-carboxylic ligands, *Inorg. Chem. Comm*., 2018, **93**, 29.

12. L.-L. Luo, X.-L. Qu, Z. Li, X. Li, H.-L. Sun, Isostructural Lanthanide-Based Metal-Organic Frameworks: Structure, Photoluminescence and Magnetic Property, *Dalton Trans.*, 2018, **47**, 925.

13. K. Zheng, Z.-Q. Liu, Y. Huang, F. Chen, C.-H. Zeng, S. Zhong, S. Weng Ng, Highly luminescent Ln-MOFs based on 1,3-adamantanediacetic acid as bifunctional sensor, *Sens. Actuators B*, 2018, **257**, 705.

14. Z.-P. Zhao, K. Zheng, H.-R. Li, C.-H. Zeng, S. Zhong, S. Weng Ng, Y. Zheng, Y. Chen, Structure Variation and Luminescence of 3D, 2D and 1D Lanthanide Coordination Polymers with 1,3-Adamantanediacetic Acid, *Inorg. Chim. Acta*, 2018, **482**, 340.

15. F.-N. Shi, M. L. Pinto, D. Ananias, J. Rocha, Structure, topology, gas adsorption and photoluminescence of multifunctional porous RE3+-furan-2,5-dicarboxylate metal organic frameworks, *Microporous Mesoporous Mater*., 2014, **188**, 172.

16. C. Chen, X. Zhang, P. Gao, M. Hu, A Water Stable Europium Coordination Polymer as Fluorescent Sensor for Detecting Fe3+, CrO4 2- , and Cr2O7 2- Ions, *J. Solid State Chem*., 2018, **258**, 86.

17. S. Zhang, Y. Yang, Z.-Q. Xia, X.-Y. Liu, Q. Yang, Q. Wei, G. Xie, S.-P. Chen, S.-L. Gao, Eu-MOFs with 2-(4-Carboxyphenyl)imidazo[4,5-f]-1,10- phenanthroline and Ditopic Carboxylates as Coligands: Synthesis, Structure, High Thermostability, and Luminescence Properties, *Inorg. Chem.*, 2014, **53**, 10952.

18. Y. Wei, R. Sa, Q. Li, K. Wu, Highly stable and sensitive LnMOF ratiometric thermometers constructed with mixed ligands, *Dalton Trans*., 2015, **44**, 3067.

19. G.-X. Guan, X. Liu, Q. Yue, E.-Q. Gao, Homochiral Metal−Organic Frameworks Embedding Helicity Based on a Semirigid Alanine Derivative, *Cryst. Growth Des.*, 2018, **18**, 364.

20. R. An, X. Wang, H.-M. Hu, Z. Zhao, C. Bai, G. Xue, Controllable synthesis of four series of lanthanide coordination polymers: synthesis, structures, luminescent and magnetic properties, *CrystEngComm*, 2015, **17**, 8289.

21. A. Thirumurugan, S. Natarajan, Yttrium coordination polymers with layered structures, *Solid State Sci*., 2004, **6**, 599.

22. A. Thirumurugan, S. Natarajan, Synthesis, structure and luminescent properties of yttrium benzene dicarboxylates with one- and three-dimensional structure, *Dalton Trans*., 2004, **2004**, 2923.

23. H. Zhao, X.-X. Sun, H.-M. Hu, R. An, M.-L. Yang, G. Xue, Syntheses, Structures and Luminescent Properties of Lanthanide Coordination Polymers Assembled from Imidazophenanthroline Derivative and Oxalate Ligands, *J. Solid State Chem*., 2017, **245**, 67.

24. D. Ma, X. Li, R. Huo, A high-efficiency white light-emitting lanthanide– organic framework assembled from 4,40 - oxybis(benzoic acid), 1,10-phenanthroline and oxalate, *J. Mater. Chem. C*, 2014, **2**, 9073.

25. S. Zou, Q. Li, S. Du, Efficient and tunable multi-color and white light Ln-MOFs with high luminescent quantum yields, *RSC Adv*., 2015, **5**, 34936.

26. Y. Wei, Q. Li, R. Sa, K. Wu, A white-light-emitting LnMOF with color properties improved via Eu3+ doping: an alternative approach to a rational design for solid-state lighting, *Chem. Commun*., 2014, **50**, 1820.

27. S. Song, X. Li, Y.-H. Zhang, White light emission of an Eu(III)-doped Gd(III) complex with 3-sulfobenzoate and 1H-imidazo[4,5-f][1,10]- phenanthroline, *Dalton Trans*., 2013, **42**, 10409.

28. R. An, H. Zhao, H.-M. Hu, X. Wang, M.-L. Yang, G. Xue, Synthesis, Structure, White-Light Emission, and Temperature Recognition Properties of Eu/Tb Mixed Coordination Polymers, *Inorg. Chem*., 2016, **55**, 871.

29. S. Song, X. Li, Y.-H. Zhang, R. Huo, D. Ma, White light emission by a lanthanide doped Sm(III) framework constructed from 4-sulfobenzoate and 1H-imidazo[4,5-f][1,10]-phenanthroline, *Dalton Trans*., 2014, **43**, 5974.

30. J.-J. Li, T.-T. Fan, X.-L. Qu, H.-L. Han, X. Li, Temperature-induced 1D lanthanide polymeric frameworks based on Ln_n(n= 2,2,4,6) cores: Synthesis, crystal structures and luminescence properties, *Dalton Trans*., 2016, **45**, 2924.

31. Y.-E. Cha, X. Li, D. Ma, R. Huo, Lanthanide Complexes Assembled from 3-Fluorophthalate and 1,10-Phenanthroline: Syntheses, Crystal Structure, Photoluminescence, and White-Light Emission, *Chem. Eur. J*., 2014, **2014**, 2969.

32. M. Fang, Z. Chen, K.-W. Yin, X.-M. Kang, H. Xu, Novel Lanthanide Coordination Polymers with Eu-compound exhibits Warm White Light Emission: Synthesis, Structure, and Magnetic Properties, *Inorg. Chem. Comm*., 2016, **70**, 51.

33. Y.-Y. Liang, L.-L. Xue, H.-M. Hu, L.-N. Zheng, X. Wang, G. Xue, Syntheses, structures, fluorescence sensing properties and white-light emission of lanthanide coordination polymers assembled from imidazophenanthroline derivative and isophthalate ligands, *J. Solid State Chem*., 2019, **276**, 6.

34. Q.-W. Xu, G. Dong, R. Cui, X. Li, 3D lanthanide-coordination frameworks constructed by a ternary mixed-ligand: crystal structure, luminescence and luminescence sensing, *CrystEngComm*, 2020, **22**, 740.

35. J. Liu, W. Sun, Z. Liu, White-Light Emitting Materials with Tunable Luminescence based on Steady Eu (III) doping Tb (III) Metal-Organic Frameworks, *RSC Adv*., 2016, **6**, 25689.